J Solid State Electrochem (2012) 16:901–909
DOI 10.1007/s10008-011-1456-y

ORIGINAL PAPER

Polymeric membranes conditioning for sensors applications: mechanism and influence on analytes detection

Ana Rosa Lazo Fraga · Josefina Calvo Quintana · Giovanni Li Destri · Nicoletta Giamblanco · Roberta Grazia Toro · Francesco Punzo

Received: 8 March 2011 / Revised: 30 May 2011 / Accepted: 3 June 2011 / Published online: 11 June 2011

Abstract In this work, we studied an ion-exchange membrane based on an inert polymer skeleton in which it is dispersed and anchored a molecule with charged groups able to discriminate and bind positive or negatively charged ions present in a sample. In order to be ready to work, electromembranes need a complex procedure called activation or conditioning. Although most of the known literature looks at the subject from an electrochemical point of view, we put forward a structural approach. Membrane conditioning, in fact, is considered a required step to improve sensor performances and to allow the collection of reproducible data. Even if this operation is carefully followed by all the operators working with sensors equipped with a membrane, it looks like that a thoroughly explanation of the working mechanism and a detailed balance of cost and gains has still not been carried out. As a consequence, we suggest a bulk or membrane approach, where the landscape is mainly characterized by the long-range structure of the membrane itself. Our findings suggest that membrane conditioning has to be carried out carefully and the advantages of this pre-treatment can be appreciated especially for very low concentration measurements. The need for the conditioning mainly results from the necessity of a complete permeation of all the different tortuous channels constituting the membrane itself.

Keywords Polymeric membranes · Electromembranes conditioning · Ion-selective electrodes · Morphological analysis · Amorphous materials

A. R. Lazo Fraga
Instituto de Materiales y Reactivos (IMRE),
Universidad de La Habana,
10400 Havana, Cuba

A. R. Lazo Fraga · G. Li Destri · N. Giamblanco · F. Punzo (✉)
LAMSUN and CSGI at Dipartimento di Scienze Chimiche,
Università degli Studi di Catania,
Viale Andrea Doria 6,
95125 Catania, Italy
e-mail: fpunzo@unict.it

J. Calvo Quintana
Dipartimento di Scienze e Tecnologie Chimiche,
Università di Roma Tor Vergata,
Via della Ricerca Scientifica 1,
00133 Rome, Italy

R. G. Toro
CNR-Istituto per lo Studio dei Materiali Nanostrutturati,
P.O. Box 10 Monterotondo Stazione, 00015 Roma, Italy

Present Address:
N. Giamblanco
Nanochemistry and Molecular Systems, University of Liege,
B6 Sart-Tilman,
4000 Liege, Belgium

Introduction

Electromembrane processes find their applications in many industrial fields like water desalination or purification, not only from chemicals, but also for high-quality raw material for biotechnological use. Among all the possible electromembrane applications, the ones on sensors, microsensor and biosensors are probably the most intriguing for their technological potentialities. Sensors are widely used nowadays to screen and detect the presence of very small quantities of chemicals or class of chemicals [1]. Their study experienced a dramatic momentum in the last years [2] due to the vast range of applications where their usage could be of great help [3, 4]. We focused our attention on potentiometric microsensors, made of a transducer and an ion-sensitive polymeric membrane constituted by continu-

ous layers acting as a permselective hindrance [5]. The ingredients of electromembranes vary, depending on membrane types. The membrane itself is not set up with any internal standard [6]. The components of each layer are a supporting skeleton—such as a PVC matrix—a highly specific ion sensitive and selective receptor—often called ionophore—and, finally, a plasticizer used to avoid any possible leaking of ionophore from the polymeric matrix. All these sensors need a so-called conditioning—or activation—procedure, consisting of their previous contact with the sample to be checked as to get them ready to operate. In previous works [7, 8], we made a first basic approach to describe the interaction mechanism of the ionophore with ions. This is what we call the molecular approach as it shed light, at the atomic level, over the interaction between the ionophore and the ions present in the sample to be measured. The present work deals instead with the possibility to describe the conditioning process from the polymeric membrane or bulk point of view: this required step is in fact critical for the sensor's fine working, but a complete and clear explanation of its mechanism and the reasons that make it so necessary are still opaque [9–11]. Throughout this paper, we referred to an ion-exchange heterogeneous membrane.

The basic properties of these membranes are mainly due to their chemical composition and the concentration of the ionophore. Mechanical, chemical and thermal stability of the membrane are affected by its chemical composition, while permselectivity, mechanical stability and the degree of swelling—actually also related to the mechanical stability of the membrane—vary with the ionophore type and concentration [12–14]. To ensure an efficient and complete contact between the sample solution and the ionophore dispersed in the membrane, the latter has to be wetted. Presumably, this is necessary to allow the solution to penetrate in all the tortuous channels that made the membrane architecture, so to provide the complete contact with the transducer. Up to now, most of the literature regarding the conditioning phenomenon is inspired by either a classical electrochemical point of view [15–18] or on local equilibrium [19–21] or non-equilibrium models [22–24]: they interpret the need for activation in terms of interfacial potentials and diffusion. In this framework, we aimed to unravel the conditioning mechanism and its effect on the membrane efficiency. We characterized the bulk polymeric membrane by means of quartz crystal microbalance with dissipation monitoring (QCM-D), thus allowing the quantification of the adsorption process; by means of X-ray diffraction (XRD), to determine the structural arrangement of active molecules within the polymeric matrix. We also studied the membrane surface, by means of atomic force microscopy (AFM) and field emission scanning electron microscopy (FESEM), to verify any morphological surface changes at nanoscopic level induced by conditioning. We, therefore, found that conditioning induces clear structural rearrangements which are necessary for high-efficiency microsensors.

Experimental

Materials

1-Furoyl-3,3-diethylthiourea (F3DET) was synthesized in the Organic Materials Laboratory of the Institute of Materials and Reagents of the University of Havana, Cuba. Fifteen milligrammes of F3DET, used as ionophore, were added to 184.6 mg of tributylphosphate (TBP) from Aldrich—used as plasticizer, to avoid demixing between the polymeric matrix and the active F3DET molecules—under stirring. One hundred milligrammes of PVC (Aldrich) were added and, to the still viscous and non-homogeneous solution, were added from 3 to 4 mL of tetrahydrofuran (THF) of analytical grade from Merck, to dissolve and to homogenize the membrane components. The $Pb(NO_3)_2$ (Aldrich) solutions were prepared with concentration varying from 10^{-5} to 1.0 M in Millipore water. The solutions were also degassed by sonication for 30 min to prevent the formation of air bubbles on the QCM-D electrodes.

QCM-D

F3DET films were deposited by spin coating technique at 3,000 rpm for 1 min by spreading three drops of the concentrated membrane solution on a gold-covered quartz sensors (Q-Sense AB, Gothenburg, Sweden). Although the membrane setup for sensor needs is commonly made by casting, the spin coating technique was chosen to ensure a complete and homogenous coverage of the QCM-D sensor, which is a key factor for this kind of analysis. AT-cut 5-MHz crystals coated with an evaporated gold film were cleaned by treating with a mixture of H_2O_2, NH_4OH and H_2O (ratio, 5:1:1 [*v*/*v*/*v*]) heated at 70 °C. After 10 min, the crystals were rinsed with Millipore (MQ) water and dried in nitrogen. Soon after they underwent 10 min UV-O_3 treatment and they were rinsed with MQ and dried once again with blown N_2. Once deposited, all the thiourea films were aged in air 4 days and three of them also one night in a $Pb(NO_3)_2$ 10^{-2} M water solution. All the aged crystals were investigated by using the QCM-D technique, which is surface sensitive, with a sensitivity of less than 1 ng/cm^2. The quartz crystal, consisting of a sensor with electrodes on each side, is mounted in a detection cell; when an AC voltage is applied across the electrodes, the crystal oscillates at its 5-MHz resonant frequency. Changes of resonance frequency (Δf) of quartz

crystal were measured and are caused by the adsorption or desorption of molecules from solution onto the sensor surface. The change in dissipation energy loss of the crystal (ΔD), which is directly connected to the viscoelastic properties of the deposited film, was also determined. The AT-cut quartz crystal, oscillates in a thickness-shear mode and the oscillation of the crystal surface gives rise to an exponentially decaying shear wave into the liquid [25]. The decay length of this shear wave δ, corresponding to the distance into the liquid where the amplitude of the shear wave has fallen by a factor e, is

$$\delta = \sqrt{\frac{2\eta_1}{\pi f \rho_1}} \tag{1}$$

where η_l and ρ_l are the shear viscosity and density of the liquid and f is the quartz resonator frequency [26]. A set of five crystals were monitored; changes in the resonant frequency and dissipation were measured for the coated crystals oscillating in water at 25 °C for an amount of time similar to the one really needed by the sensor, thus simulating the sensor working environment. In order to mimic the sensor behaviour with respect to real samples, the conditioning process was performed with a $Pb(NO_3)_2$ 10^{-2} M solution, soon after the crystals and the membranes were rinsed again with water as to make the whole system ready to respond to Pb^{2+} ions. The collected data were analysed by QTools software (Q-Sense, BiolinScientific, Sweden).

FESEM

Surface morphology was examined by FESEM using a ZEISS SUPRA 55 VP microscope, equipped with the INCA Energy Oxford solid-state detector for energy-dispersive X-ray analysis.

AFM

Topographical images were taken using a Digital Instruments (DI) Nanoscope IIIA (Veeco) with 100×100 μm scanner under ambient conditions. Images were acquired in tapping mode (TM) by employing silicon cantilevers with resonance frequency ~260 kHz (Veeco NanoProbe Tips RTESP). The roughness estimation was made on scan areas of 8×8 μm^2 in terms of standard deviation of height (Rq) defined as

$$R_q = \sqrt{\frac{\sum (Z_i)^2}{n}} \tag{2}$$

where Z_i is the current height value and n is the number of points within the AFM image.

XRD

The X-ray diffraction measurements of both powder and membrane were collected at room temperature on a Rigaku Ultima IV type III diffractometer (Rigaku, Tokyo, Japan) in the parafocusing geometry by using a Kα wavelength emitted by a Cu anode. The umbrella divergence of both incident and diffracted beams were reduced with two 5° soller slits. A high-speed solid-state detector, D/Tex Ultra, was used for the membrane: the high sensitivity of this detector, 100 times higher than a conventional scintillation detector [27], increased the observed signal to noise ratio and, thus, allowed the observation of the characteristic amorphous humps. Several checks were made to ensure that the F3DET X-ray powder pattern, collected with a scintillation detector, corresponded to the non-damaged microcrystalline structure of the compound. On the other hand, in the lack of a possible comparison, the ultra-fast detector was used for the membranes. This allows the data collection avoiding the possible damage of the sample as a consequence of its long exposure to X-rays.

Results and discussion

The type of system we are dealing with is constituted by a membrane of thickness d separating two type of electrolytes: while the theory of membranes often sees the membrane separating two second kind conductors, in ion-selective electrodes (ISE) we are considering a membrane separating a sample solution on one hand, slowly wetting and permeating the sensor membrane and, on the other hand, a first kind conductor, i.e. a copper slice transducing the electrical signal to the bulk of the electrode. Generally, the systems are classified as non-osmotic or osmotic. Our sensors belong to the first class as the presence of a metal contact at the base of the membrane actually makes the possible osmotic pressure become null. The state of equilibrium for this system is achieved when all ion fluxes vanished. It corresponds to

$$J_{+i} = J_{-i} = 0 \tag{3}$$

where J_+ and J_- are the fluxes corresponding to positively and negatively charged species, respectively. If the membrane were permeable to all ions, the equilibrium would be reached when the concentration differences become null. As we need a non-null potential difference the membrane must be semi-permeable or better permeable to some ions only. This is our case: a network formed by the inert polymer matrix—PVC in our case—binds several (partially) [7] negatively charged F3DET molecules which actually exclude the permeation of any anion present in solution, thus allowing, on the other hand, the interaction with cations. In

such a case, the well-known Nernst equation describes correctly the potential difference on the two sides of the membranes.

The Nernstian behaviour of the electrode is ensured only above the sensor detection limit. As already reported by Bakker [28], ISE's key characteristic is selectivity. To lower the detection limit, both in the case of easily detectable primary ions or not [29, 30], and to ensure a reproducibility in the measurement, the conditioning procedure seems to be needed.

QCM-D

The QCM-D setup allowed us to simulate the sensor behaviour by sinking the gold contact on which the membrane was deposited, directly in the solution where the sensor normally works. In Fig. 1, the QCM-D curves for the membrane deposited on a gold sensor oscillating in water (A1), without being previously conditioned, are reported. The frequency shifts for the third, fifth and the seventh overtones (corresponding to 15, 25 and 35 MHz) are shown. A fast increase of Δf (41.0±5.0 Hz) was measured in water for the membrane sensor stabilized 4 days in atmospheric ambient, i.e. what we called the non-activated membrane.

The analysis was carried out for a time of the same order of magnitude of the working conditions of the real electrodes. The results suggested that the experimental time was too short and did not allow the system to go to equilibrium, as evidenced by the lack of a plateau in the curve. It must be noted that the positive shift of frequency is associated with desorption processes. They could be linked to the removal of unbound low-molecular-weight fraction of polymer at the membrane surface. The sensor membrane stabilized one night in Pb aqueous solution, i.e the so-called activated membrane, showed that a small but well-defined adsorption occurred. In particular, the Δf decreases about −5.3±0.3 Hz and ΔD increases $0.4\pm0.1\times10^{-6}$ after 10 min of oscillations in the solution until equilibrium was achieved. After that, the membrane spent one night in the lead nitrate solution; the negative frequency shift indicates that some solution adsorption at the inner part of membrane took place, thus producing a viscoelastic damping of the sensor. Since adsorption does not vary the dissipation behaviour, the Sauerbrey equation [31], valid for rigid films can be employed to estimate the amount of adsorbed species, thus, evidencing an uptake of 0.3 ng. The membrane swelling cannot be accounted for this effect: the adsorption involved mainly the cations in solution.

We are, therefore, dealing with two different systems: the former, A, not conditioned, that did not reach the equilibrium, at least within the normal electrode working times, indicating that an uneven or incomplete interaction with the solution took place; the latter, B, that clearly shows the progressive uptake of solution, even in the bulk, and that well behaved as a sensor membrane even within the typical working times. On the other hand, allowing the non-activated membrane a longer time to eventually reach the equilibrium, it would have mimicked the same experimental condition corresponding to membrane activation. The solution, in fact, needs time to enter a dry, rigid and non-activated membrane in analogy with the behaviour of a liquid on a dry sponge. Only a soaked sponge allows a liquid to enter thoroughly its pores and permeate the sponge. A dry sponge instead, is almost impermeable to any liquid spilt on its surface, i.e. in a dry sponge; the liquid will almost bounce off of its surface, wetting the surface only. A non-activated membrane acts like a dry sponge: it is not so willing to absorb water and, a part from its surface, it mainly remains dry. It is, therefore, unable to work as a sensor's membrane. A different behaviour was seen in the conditioned membrane. It is already soaked with the solution solvent and therefore ready to host in its open pores other solvent: this is exactly the most favourable condition to let a complete and thorough exchange between the membrane ad the solution to be tested, as requested by a sensor.

In Fig. 2, the QCM-D measurements for the F3DET membranes in response to $Pb(NO_3)_2$ at successive concentrations are reported. The decreasing steps, clearly visible in

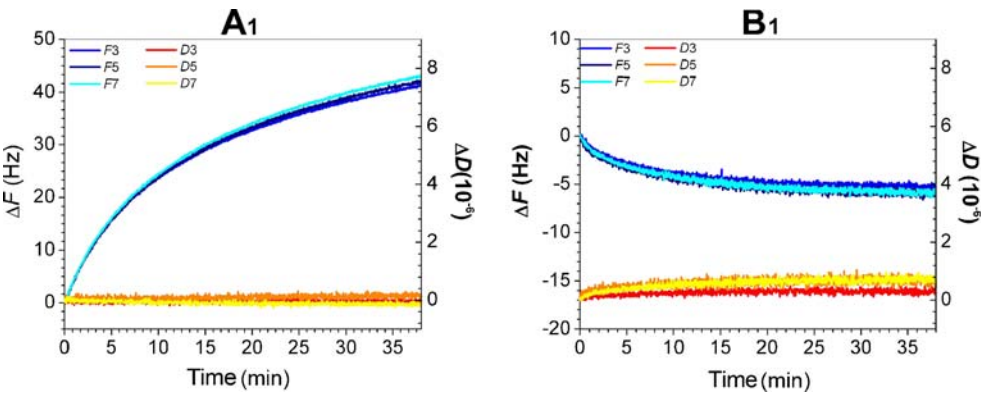

Fig. 1 QCM-D curves of frequency and dissipation shifts for thiourea membrane stabilized in air (*A1*) on the left and one night in a 10^{-2}-M $Pb(NO_3)_2$ solution (*B1*) on the right, respectively, and both oscillating in water. The different frequency shifts for the third, fifth and the seventh overtones (corresponding to 15, 25 and 35 MHz) and the corresponding dissipations are shown

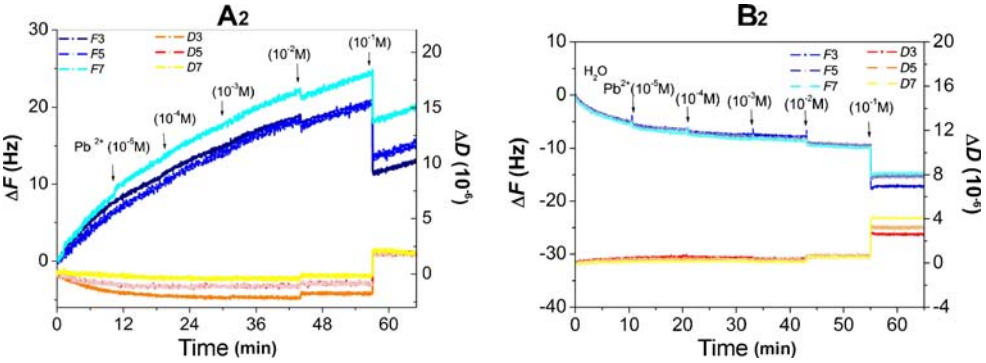

Fig. 2 QCM-D curves of frequency and dissipation shifts for thiourea membranes stabilized in air (*A2*) on the left and in a 10^{-2} M $Pb(NO_3)_2$ solution (*B2*) on the right, respectively, and both oscillating in water. The different frequency shifts for the third, fifth and the seventh overtones (corresponding to 15, 25 and 35 MHz) and the corresponding dissipations are shown

the figure, correspond to the different additions of growing concentration of $Pb(NO_3)_2$ solutions to the membrane in the measuring cell. They were performed each 12 min, i.e. within the normal working times. The response of the membranes to Pb^{2+} ions, one stabilized in atmospheric ambient (A2) and the other one conditioned in a 10^{-2} M Pb $(NO_3)_2$ solution (B2) were once again different. In particular, positive Δf were measured for (A2), in response to a salt concentration of $Pb(NO_3)_2$ 10^{-5}, 10^{-4} and 10^{-3} M. When passing to more concentrated Pb^{2+} solutions, i.e. 10^{-2} and 10^{-1} M, the frequency decreased and dissipation increased at first. They then changed their trends increasing again, thus showing that some adsorption–desorption took place. As for A1, the system did not reach the equilibrium, and as a consequence, the only reasonable consideration is that the membrane, without the conditioning step, is not ready to work. On the other hand (B2), the response to the $Pb(NO_3)_2$ was fast even at low concentration -10^{-5} M, inducing a rapid decrease of frequency and an increase of the dissipation factor already observed for B1. This is an evidence that an activated membrane shows its sensitivity even to low or very low concentrations. Moreover, there is a bigger frequency decrease by raising the concentration of lead solutions, thus, indicating that the more concentrated they are, the higher the adsorption. This is the basis of the working mechanism of the sensor's membrane whose electrochemical response is selective towards the amount of analyte to detect [32, 33]. Furthermore, the same structural considerations made for B1 can be done. These results clearly confirm the different properties and attitudes of the membrane before and after water conditioning.

XRD

In order to highlight any membrane structural change at the atomic level, the X-ray diffraction patterns of the non-activated and activated membranes were collected, as specified in the experimental section. In Fig. 3, we report the diffraction patterns of the non-activated and activated membrane, as compared with the corresponding powder diffraction pattern of the ionophore molecule alone. A detailed X-ray study of the single crystal, as well as a comparison of the single crystal results with the X-ray powder diffraction, was already performed [7, 8]. The abovementioned diffraction patterns evidenced, at a glance, the disorder evolution while passing from the ionophore powder alone (in black) to the non-activated (in red) to the activated membrane (in blue), respectively. There were no significant differences among the membrane diffractograms, as the difference in the overall intensity can be due to the presence of solvent in the membrane, thus, causing an overall disarrangement. Furthermore, the qualitative humps distribution reminds that of the ionophore alone; this latter shows well-resolved peaks, while the membrane, as a consequence of the dispersion of the ionophore crystallites in a non-crystalline polymeric matrix, exhibits the characteristic peak broadening of disordered materials. They become, according to literature [34], large and undefined humps. Moreover, similarly to typical amorphous samples, few broad signals, corresponding to the average molecular radial distribution [35], appear. The position of the maxima of such signals can be used to have a deeper

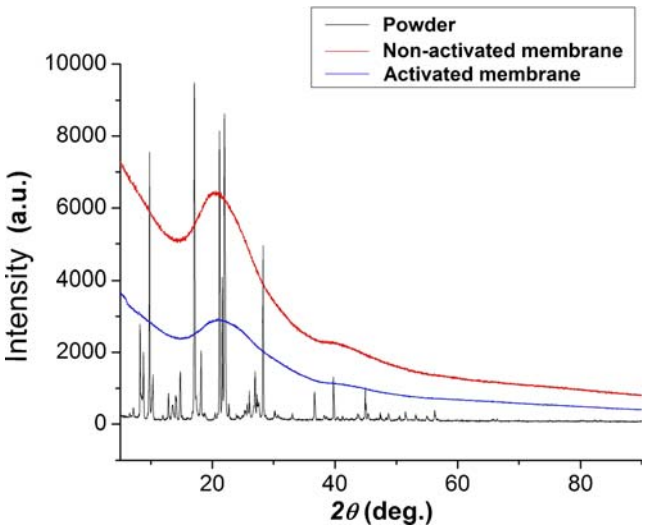

Fig. 3 X-ray diffraction patterns of F3DET powder, non-activated and activated membrane

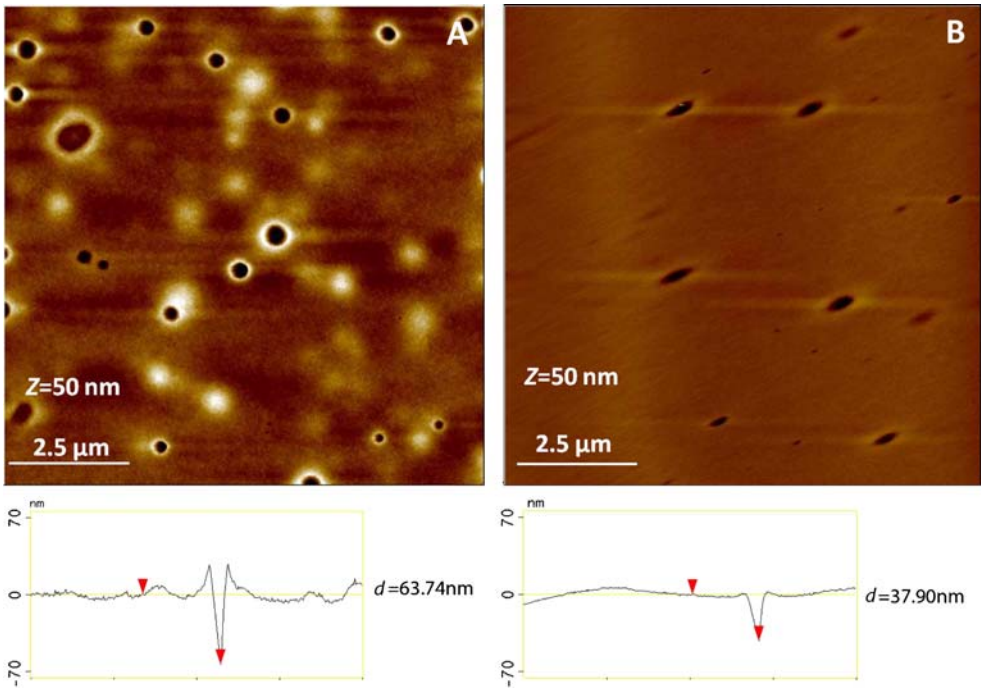

Fig. 4 Tapping mode AFM images (8×8 µm) obtained in air on the surface of spin-coated F3DET membrane stabilized in air 4 days (**a**) and one night in water (**b**). Below each image, the corresponding topographical cross section is reported. The value beside each cross section represents the *vertical distance* between the *two red arrows*, i.e. the pore depth

insight concerning the molecular arrangement of F3DET inside the membrane. In particular, since the maxima of these signals are located at angles where the main groups of diffraction peaks of crystalline F3DET appear, we can infer that the structural arrangement of F3DET within the polymeric matrix resembles the crystalline one even if with an extremely shorter range. We can assume, therefore, that the membrane did not undergo any dramatic structural change, at the atomic level, at least in passing from non-activated to activated. The solvent, water in our case, seems to be responsible for membrane deformation, but did not actually cause a structural rearrangement of the membrane ingredients. The progressive lowering of the amorphous diffraction profile and its overall intensity decrease, passing from the non-activated (red curve) to the activated membrane (blue curve), suggests, on one hand, the presence of a less crystalline or less ordered membrane, on the other, a substantial reduction of the number of scattering centres, i.e. in our case, the ionophore crystallites.

AFM

Figure 4 shows tapping mode AFM images measured in air on the surface of the spin-coated membrane, stabilized 4 days in atmospheric ambient (A) and one night in a Pb $(NO_3)_2$ 10^{-2} M solution (B). Both films showed random holes with circular rims of about 0.3 and 0.5 µm diameter, respectively. They are the result of the evaporation of THF

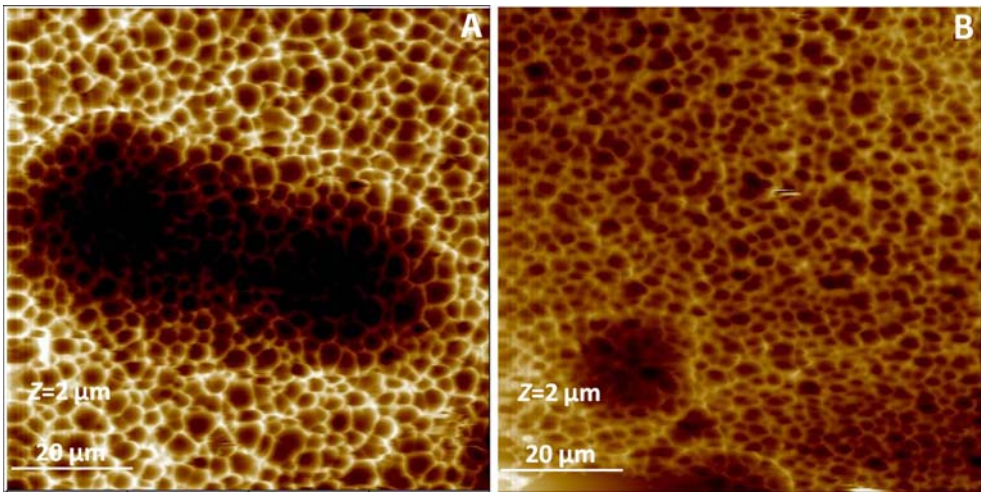

Fig. 5 Tapping mode AFM images (8×8 µm) obtained in air on the surface of casted F3DET membrane stabilized in air 4 days (**a**) and one night in a Pb $(NO_3)_2$ 10^{-2}-M solution (**b**)

Table 1 Mean diameter and mean depth of pores belonging to spin coated and casted membranes without and with conditioning, respectively

	Spin coated		Casted	
	Non-activated	Activated	Non-activated	Activated
Mean diameter	339.2±119.9 nm	351.0±148.8 nm	3.36±1.41 μm	3.05±2.10 μm
Mean depth	77.5±22.9 nm	36.6±2.6 nm	815.6±85.8 nm	489.0±23.5 nm

Please note that the average pore size increases 10^3 times passing from a spin-coated to a casted membrane, as highlighted by the different measurement units associated

from the bulk of the membrane. THF, in fact, tends to evaporate quite fast at room temperature. While the solvent evaporation is allowed on the membrane surface, the solvent trapped below the surface, although ready to evaporate, creates bubbles below the surface. These bubbles try to come out of the surface, puncturing the membrane or creating a path during their way to the surface: this is one of the possible reasons for the porous nature of the membrane. Alternatively, a negligible part of them could be kept inside the membrane itself and possibly being released during the membrane swelling. The roughness of the thiourea membrane stabilized one night in $Pb(NO_3)_2$ water solution was less than the other one with a *R*q value of 1.83±0.07 and 5.57±0.23 nm, respectively. The disappearance of bumps, as a consequence of the membrane washing that takes place during the conditioning process, together with the decrease of the mean depth of pores, which is 77.5±22.9 nm before the conditioning and 36.6±2.6 nm after it, can be accounted for the overall mean roughness decrease. A similar trend was also observed when casted membranes, i.e. "really working membranes", were analysed (Fig. 5). This is an evidence that this behaviour does not depend on how the membrane was deposited. As expected, a porous sponge-like morphology is detected on both as-prepared and conditioned samples, but markedly different values of roughness were measured. In particular, the non-activated membrane showed *R*q=222.40±22.03 nm, while the conditioned one showed *R*q=149.73±21.26 nm. The solution absorption process was indeed responsible of blowing up the membrane, thus, smoothing its surface and narrowing its pores, similarly to the surface of an inflated balloon, as a consequence of a considerable hydration of the membrane, while no effect on the pores mean diameter was observed as reported in Table 1. The process starts from the membrane surface, letting the solvent entering from the pores and then slowly penetrating in the membrane bulk via the tortuous channels constituting the membrane: it ensures a homogenous behaviour of the membrane and a quite complete contact of the solution with the sensor's components, with a particular care for the ionophore and the transducer. The abovementioned change in mean roughness evidenced by AFM measurements is consistent with the above proposed model of soaked sponge.

FESEM

Figure 6 shows FESEM images of a non-activated and activated membrane, respectively. Both membrane surfaces show an almost concordant picture as compared with AFM ones: a rough membrane surface, with bumps and lumps of different diameters, probably resulting from solvent evaporation. At the same time, FESEM investigation revealed some differences as compared to that observed during AFM measurements. In particular, the surface of the non-activated membrane is characterized by an homogeneous distribution of small crystallites having a block shape. Their shape was in agreement with the crystal habit described for the F3DET single crystal. [7] This is an evidence of the thiourea presence on the membrane surface, stuck on it, as a

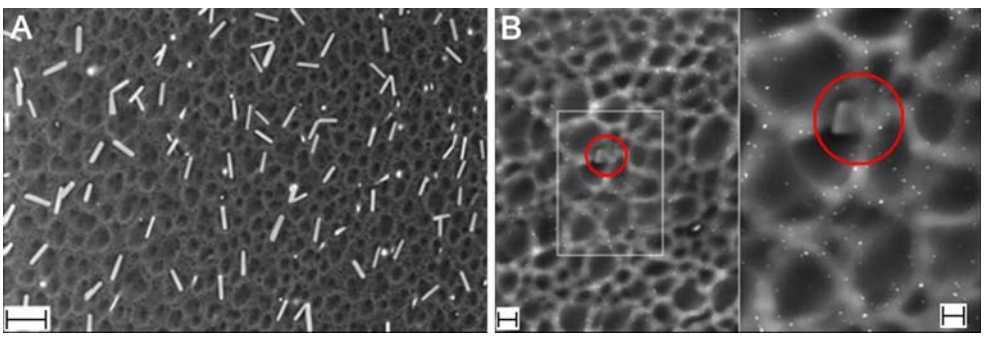

Fig. 6 FESEM images of spin-coated F3DET membrane stabilized in air 4 days (**a**) and one night in a $Pb(NO_3)_2$ 10^{-2}-M solution (**b**). The *inset* is magnified in the *right part* of the figure (**b**): small white $Pb(NO_3)_2$ grains are clearly visible as well as (*circled in red*) an ionophore crystallite stuck in the membrane itself. Data scale is 10, 2, 1 μm, respectively

consequence of the plasticizer (TBP), whose main duty is avoiding the membrane ingredients leaking in the solution to be measured. Moreover, the high magnification of the FESEM image of the non-activated membrane (Fig. 6a) shows also the presence of some small grains which looked like embedded in the pores of the PVC membrane. As soon as the membrane is sunk one night into the $Pb(NO_3)_2$ 10^{-2} M solution to perform the activation process, its surface changed: no ionophore crystallites were visible on the surface of the activated membrane (Fig. 6b) because of the washing effect of the solution. At the same time, the small grains indicating the inclusion of ionophore inside the membrane were still evident, even if their number sensibly decreased as compared to that observed for the non-activated membrane. These results indicated that a progressive cleaning-out process of the ionophore took place from the first step of the activation process. Furthermore, in Fig. 6b, small white grains came in sight: these are the evidence of $Pb(NO_3)_2$ stuck into, or deposited over the membrane as a consequence of the activation process. Moreover, in the right side, a further magnification allows the detection (circled in red) of another ionophore crystallite trapped into the membrane.

Conclusions

The conditioning step in the light of the present study is not only an electrochemical habit suggested by decades of use. QCM-D measurements confirmed the good behaviour only of an activated membrane for sensor purposes. The morphological analysis, performed by means of AFM highlighted the membrane swelling and its change in average roughness on one hand, and the progressive washing of the ionophore as a consequence of the continued use of the membrane, noticed by means of FESEM images, on the other hand. X-ray diffraction proved that no rearrangements at the atomic level took place passing from the non-activated to the activated membrane, but confirmed the FESEM hypothesis of a progressive crystallites diminishing in the membrane. The abovementioned swelling is the key process that allows the membrane to enter thoroughly in touch with the solution to be measured, and this process, a necessary prerequisite for the successful membrane operation, must not be confined to the surface only, but should involve the whole membrane. The ionophore crystallites presence was not evidenced by the AFM analysis as the membrane analysis was carefully performed over the area without crystallites to avoid any possible damage to the fragile AFM piezoelectric scanner. Furthermore, the FESEM image after conditioning confirms the X-ray hypothesis: the number of crystallites diminished as the membrane washings proceeded, i.e. from the X-ray point of view, the scattering centres lowered and the overall signal intensity dropped. We can, therefore, imagine that as far as the membrane undergoes several "washes" throughout its whole working life, one after the other, all the ionophore crystallites dispersed in the membrane—not only on its surface—will be ripped out from the membrane by dissolving in the aqueous media, until no ionophore can be traced. This is of course the last stage of the membrane operating life: without any ionophore the membrane cannot work anymore.

Moreover, a possible formation of a water layer over the transducer was accounted as a consequence of over-conditioning [36–38]. This can cause an excessive and unwanted local dilution of the solution to be measured. As a consequence, it is evident that although a complete conditioning is requested to get a fully working membrane, this step has to be performed with care and bearing in mind that an over-conditioning will cause a faster membrane depletion.

Acknowledgements Authors wish to thank Prof. G. Marletta for the helpful discussions. ARLF acknowledges CSGI financial support.

References

1. Bakker E, Pretsch E (2007) Angew Chem Int Ed 46:5660–5668
2. Bobacka J, Ivaska A, Lewenstam A (2008) Chem Rev 108:329–351
3. Dewitte K, Stöckl D, Thienpont LM (1999) Lancet 354:1793–1794
4. Kang TM, Hilgemann DW (2004) Nature 427:544–548
5. Durst RA, Baumner AJ, Murray RW, Buck RP, Andrieux CP (1997) Pure Appl Chem 69:1317–1323
6. Alegret S (1996) Analyst 121:1751–1758
7. Lazo Fraga AR, Collins A, Forte G, Rescifina A, Punzo F (2009) J Mol Struct 929:174–181
8. Lazo Fraga AR, Li Destri G, Forte G, Rescifina A, Punzo F (2010) J Mol Struct 981:86–92
9. Konopka A, Sokalski T, Lewenstam A, Maj-Zurawska M (2006) Electroanalysis 18:2232–2242
10. Konopka A, Sokalski T, Michalska A, Lewenstam A, Maj-Zurawska M (2004) Anal Chem 76:6410–6418
11. Berezina NP, Timofeev SV, Kononenko NA (2002) J Membr Sci 209:509–518
12. Fujimura M, Hashimoto T, Kawai H (1982) Macromolecules 15:136–144
13. Gebel G (2000) Polymer 41:5829–5838
14. Shukla R, Cheryan M (2002) J Membr Sci 198:75–85
15. Pungor E (1998) Anal Sci 14:249–256
16. Guggenheim EA (1929) J Phys Chem 33:842–849
17. Nikolskii BP (1937) Zh Fiz Khim 10:495–503
18. Eisenman G (1969) Ion Selective Electrodes, R.A. Durst (ed), NBS Special Publication 314, NBS, Washington
19. Lewenstam A (1977) The diffusion layer model in ion-selective electrodes, Ph.D. Thesis, Warsaw University, Poland
20. Hulanicki A, Lewenstam A (1977) Talanta 24:171–175
21. Lewenstam A, Hulanicki A, Sokalski T (1987) Anal Chem 59:539–1544
22. Szigeti Z, Vigassy T, Bakker E, Pretsch E (2006) Electroanalysis 13–14:1254–1265
23. Brumleve TR, Buck RP (1978) J Electroanal Chem 90:1–31

24. Sokalski T, Lingenfelter P, Lewenstam A (2003) J Phys Chem B 107:2443–2452
25. Kanazawa KK, Gordon JG (1985) Anal Chim Acta 175:99–105
26. Rodahl M, Kasemo B (1996) Sensors Actuator B Chem 37:111–116
27. Szczygiel R, Grybos P, Maj P, Tsukiyama A, Matsushita K, Taguchi T (2009) Nucl Instrum Meth A 607:229–232
28. Bakker E (1996) J Electrochem Soc 143:L83–L85
29. Bakker E (1997) Electroanalysis 9:7–12
30. Bakker E, Qin Y (1997) Anal Chem 69:1061–1069
31. Sauerbrey G (1959) Z Phys 155:206–222
32. Lazo AR, Bustamante M, Jimenez J, Arada MA, Yazdani-Pedram M (2006) J Chil Chem Soc 51:975–978
33. Lazo AR, Bustamante M, Arada MA, Jimenez J, M. Yazdani-Pedram M (2005) Afinidad 62:605–610
34. Klug HP, Alexander LE (1974) X-ray diffraction procedures for polycrystalline and amorphous materials, 2nd edn. John Wiley, New York
35. Giacovazzo C (2002) Fundamentals of crystallography. Oxford University Press, Oxford
36. Morf WE, Badertscher M, Zwickl T, Reichmuth P, de Rooij NF, Pretsch E (2000) J Phys Chem B 104:8201–8209
37. Sutter J, Pretsch E (2006) Electronalysis 18:19–25
38. De Marco R, Veder J-P, Clarke G, Nelson A, Prince K, Pretsch E, Bakker E (2008) PCCP 10:73–76